INDIAN JOURNAL OF SCIENCE AND TECHNOLOGY

*Corresponding author.

sarah2017711@gmail.com

Absorption Activity Investigation of Saturable Absorber for Dual Wavelengths in Laser Passive Q-Switching System

Sara Abdul Hussien^{1*}, Abdul-Kareem Mahdi Salih^2

1 Bio Medical Engineering, College of Engineering, University of Thi-Qar, Nasiriyah, Iraq
2 Physics Department, College of Science, University of Thi-Qar, Nasiriyah, Iraq

Abstract

Objective: The absorption activity of saturable absorber material (Cr^{+4}: YAG) for dual wavelengths (1.064 μm and 0.946 μm), simultaneously generated in same passive Q-switching system, has been investigated. **Methods:** This study utilized the mathematical model that was used in our previous study. Rung-Kutta—Fehelberge numerical method has been used to solve this mathematical model. Nd^{+3}: YAG used as an effective medium and Cr^{+4}: YAG used as a saturable absorber in the laser passive Q-switching optical system. **Finding:** When the population density of saturable absorber (n_i) increases, the steady state of photons losses occurs at advancement time and the absorption activity reaches to optical bleaching state at advancement time also (it is occurring approximately at time 35 ns from the beginning of the time of pulse construction when the $n_i = 4 \times 10^{18} cm^{-3}$, while at $n_i = 3 \times 10^{18} cm^{-3}$, approximately at time 47 ns). **Novelty:** The absorption activity of saturable absorber material for a single wavelength of photons oscillating inside the passive Q-switch laser system received attention by some studies. This study verifies or investigates from the behavior of absorption activity of saturable absorber material when encounters photons with two wavelengths oscillating simultaneously inside the laser cavity in order to obtain high power of the pulses.

Keywords: Laser; Passive Qswitching; laser; Dual wavelengths laser; Solid state lasers

1 Introduction

Dual-wavelength lasers are great interest in wide applications such as terahertz generation, biomedicine, precision measurement spectroscopy, range-finding, spectroscopy, free space communication and laser surgery[1,2]. The generation of high-power pulses by subjecting these wavelengths to optical techniques it has received the attention of researches, the passive Q-switching technique (PQS) is one of these techniques, it is depends on the presence intracavity saturable absorber material (SA)[3,4]. Laser passive Q -switching technique is a reliable approach to obtain laser pulses of the nanosecond

order [5].

The choices of SA to work in the compatibility case with the active medium (AM) very important, for this reason the absorption activity and the optical bleaching state of SA in the case of a single wavelength of photons oscillating inside the passive Q-switch laser system received attention by the studies [6,7] which was interested in studying this topic for a single wavelength. While this study focuses and investigates the absorption activity of Cr^{+4}:YAG saturable absorber towards the dual wavelengths of Nd^{+3}:YAG laser oscillating simultaneously inside the passive Q-switching system, also the time of occurrence of optical bleaching state was studied in this study.

The energy level scheme of Cr^{+4}:YAG as shown in Figure 1 [8]. The absorption of the pump wavelength occurs at the 1-3 transition. The transition 3-2 was very fast. For a material to be suitable as a passive Q-switch, the absorption cross-section of the ground state must be large, while the lifetime of the upper state (level 2) must be long enough to allow significant depletion of the ground state due to laser radiation. When an SA is inserted into a laser cavity, it appears opaque to laser radiation until the photon density is large enough to reduce the population on the ground. If the upper energy levels are sufficiently occupied, the absorber of laser radiation becomes transparent, which means the optical bleaching state of SA occurs.

Nd^{+3}:YAG crystal has been used an active medium; the energy level structure of Nd^{+3} ion in Nd^{+3}:YAG is illustrated in Figure 2 [9]. The energy level system of Nd: YAG consists of a stark split $^4I_{11/2}$, $^4F_{9/2}$ ground state and $^4F_{3/2}$ excited state. The wavelength 1.064 μm due to the $^4F_{3/2} \rightarrow ^4I_{11/2}$ transition, while 0.964 μm due to the $^4F_{3/2} \rightarrow ^4I_{9/2}$ transition. The characteristics of laser between the 4-level system and the quasi-three-level system produce a major difference. Because of small division of energy for each manifold, it is assumed that the relaxation times for the energy level within the manifold are also very small [10].
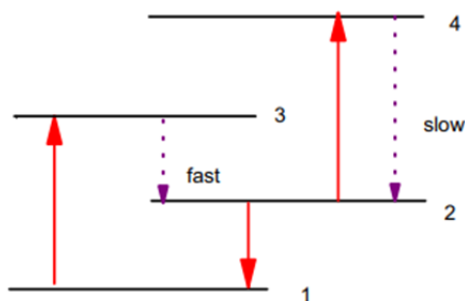
Fig 1. Energy levels scheme of Cr^{+4}:YAG [8]
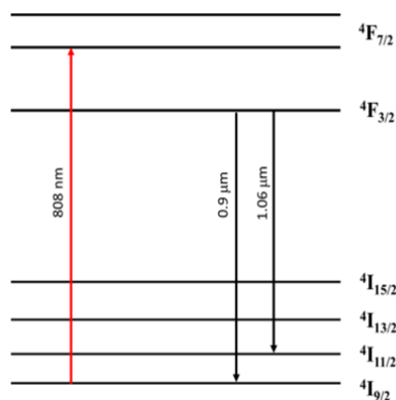
Fig 2. Energy level scheme of Nd^{+3}:YAG [9]

2 Methodology

Rate equations model[11] used in this study as the following:

$$\frac{d\varphi_1}{dt} = \varphi_1\left[K_{am1}N_{g1} - K_{sg1}n_{sg} - K_{se1}n_{se} - \gamma_{c1}\right] \tag{1}$$

$$\frac{d\varphi_2}{dt} = \varphi_2\left[K_{am2}N_{g2} - K_{sg2}n_{sg} - K_{se2}n_{se} - \gamma_{c2}\right] \tag{2}$$

$$\frac{dN_{g1}}{dt} = R_p - \gamma_{p1}K_{am1}N_{g1}\varphi_1 - N_{g1}/\tau_g \tag{3}$$

$$\frac{dN_{g2}}{dt} = R_p - \gamma_{p2}K_{am2}N_{g2}\varphi_2 - N_{g2}/\tau_g \tag{4}$$

$$\frac{dn_{sg}}{dt} = -K_{sg1}n_{sg}\varphi_1 - K_{sg2}n_{sg}\varphi_2 + n_{se}/\tau_{se} \tag{5}$$

$$\frac{dn_{se}}{dt} = K_{sg1}n_{sg}\varphi_1 + K_{sg2}n_{sg}\varphi_2 - n_{se}/\tau_{se} \tag{6}$$

Equations (1) and (2) represent the time variation of photons density of PQS pulses which are generated from λ_1, λ_2 laser respectively, (φ_1) belong to the 4-level scheme, while φ_2 belong to the 3-level scheme). Equations (3) and (4) represent the time variation of population inversion density, N_{g1} is the population inversion density (PID) of ions (cm^{-3}) between $^4F_{3/2}$ and $^4F_{11/2}$ spectrum lines. N_{g2} is the PID of ions between $^4F_{3/2}$ and $^4F_{9/2}$ spectrum lines. $K_{amj(j=1,2)} = \frac{2\sigma_{aj}l_{am}}{\tau_T}$ is the coupling coefficient between the φ_1, φ_2 photons and the ions of excited level of AM $\left(^4F_{3/2}\right)$. σ_{aj} is the emission cross sections $\left(cm^2\right)$ of AM at 4-energy level, 3- energy level schemes, l_{am} is the length of AM. $\tau_r = \frac{2l_c}{c}$ is the round-trip transit time, l_c is the cavity optical length, c is the speed of light in vacuum. Equations (5) and (6) represent the time variation of ions population in the ground and excited state respectively, $K_{sgj(j=1,2)} = \frac{2\sigma_{sg}l_s}{\tau_T}$ is the coupling coefficient between φ_j photons and the ground state ions of SA respectively, $K_{sej(j=1,2)} = \frac{2\sigma_{sej}l_s}{\tau_r}$ is the coupling coefficient between φ_j and the excited state ions of the SA respectively. $\sigma_{sgi(j=1,2)}$ sections $\left(cm^2\right)$ of excited state of SA, l_s is the length of the SA. $\gamma_{cj(j=1,2)} = \left(ln\frac{1}{R_j} + L_j\right)$ is the cavity decay rate represents the sum of losses in φ_j because of the reflectivity (R_j), absorption and scattering mechanisms in cavity (L_j). $\gamma_{pj(j=1,2)}$ is the reduction population factor equal 1,2 for four and three energy levels schemes of AM system respectively. n_{sg}, n_{se} the ions population (No. of ions density) of the ground and excited levels of SA respectively. τ_g the fluorescence lifetime of the upper laser level $\left(^4F_{3/2}\right)$, τ_{se} the lifetime of the SA. R_P is the pumping rate. The build-up time of PQS laser pulses is generally very short compared to τ_g and $R_P$time, then it is possible to neglect the terms of pumping rate and spontaneous decay of the upper laser level (terms 1 and 3 in Equations (3) and (4)) during pulse generation, so τ_{se} is very long compared the build-up time of PQS laser pulses, then it is possible to neglect the third term of Equations (5) and (6).

PQS laser pulses, then it is possible to neglect the third term of Equations (5) and (6).

The initial population inversion density (IPID) between the spectral lines $^4F_{3/2}$ and $^4F_{11/2}(N_{g01})$, $^4F_{3/2}$ and $^4F_{s/2}(N_{g02})$ can be estimated at the initial time by boundary conditions, $n_{sg} \approx n_o$ or $n_{se} \approx 0$, where $(n_i = n_{sg} + n_{se})$ is the total ions of SA. $\frac{d\varphi_j}{dt} \approx 0$ in Equations (1) and (2) because of φ_j is very low in value, then the IPID values N_{g01}, N_{g02} for laser medium can be predicted from Equations (1) and (2) respectively, as the following:

$$N_{g0j(j=1,2)} = \frac{K_{sgj}n_i + \gamma_{cj}}{K_{amj}} \tag{7}$$

The threshold population inversion (TPID) for the four and three-level schemes, N_{th1}, N_{th2} respectively, can be estimated at the time of maximum photon density (when the number of photons inside the optical laser cavity reaches the peak of the pulse) by

Equations (1) and (2). At TPID the most of the SA ions population in the excited state (n_{se}), can be regarded $n_{se} \approx n_i$ ($n_{sg} \approx 0$); then can be considered $\frac{d\varphi_j}{dt} \approx 0$.

The total photon losses (Tloss) occur by the absorption of SA, and the cavity losses (γ_c). In order to compare the population inversion density of the laser to the loss of the overall laser system, it is convenient to define the normalized loss parameter. From Equations (1) and (2), the photon losses in the overall optical system can be estimated as follows:

$$Tloss_{(\varphi_j)} = \left[\frac{K_{sgj}n_{sg} + K_{se1}n_{se} + \gamma_{cj}}{K_{amj}} \right] \tag{8}$$

Where $j = 1, 2$ for λ_1 and λ_2 respectively. estimate the total absorption activity (TAct$_{SA}$) of SA, λ_j to is equal to the absorption activity of the ground state (Act $_{sg}$) and the absorption activity of excited state (Act $_{se}$) of SA to λ_j.

$$TAct_{SA(\varphi_j)} = \left[\frac{K_{sgj}n_{sg} + K_{sej}n_{se}}{K_{amj}} \right] \tag{9}$$

The absorption activity of the SA ground state to the λ_j represented by the expression:

$$Ac_{sg(\varphi_j)} = \left[\frac{K_{sgj}n_{sg}}{K_{amj}} \right] \tag{10}$$

The absorption activity of SA excited state to the λ_j represented by the following expression:

$$Ac_{se(\varphi_j)} = \left[\frac{K_{sej}n_{se}}{K_{amj}} \right] \tag{11}$$

3 Results and Discussion

The rate Equations (1), (2), (3), (4), (5) and (6) have been solved numerically by Rung-Kutta -Fehelberg method. The input data has been used in simulation reported in Table 1:

Table 1. Input data used in simulation

Parame.	Value	Parame.	Value
σ_{a1}	$2.8 \times 10^{-19} cm^2$ [12]	σ_{sg1}	$7 \times 10^{-18} cm^2$ [13]
σ_{a2}	$5.1 \times 10^{-20} cm^2$ [14]	σ_{sg2}	$4 \times 10^{-18} cm^2$ [14]
λ_1	$1.064 \mu m$ [15]	σ_{se1}	$2 \times 10^{-18} cm^2$ [16]
λ_2	$0.946 \mu m$ [17]	σ_{se2}	$1.1 \times 10^{-18} cm^2$ [14]
γ_1	1 [4]	R_1	0.94
γ_2	2 [13]	R_2	0.99

Figure 3**a, b** show the time behavior of photon losses within the cavity of a laser system for dual pulses for two values of ions density (n_i). At the initial time, the loss may be higher due to the high absorption at that time, until a steady state is reached. From the figure, we can see that when the n_i increases, the steady state of losses occurs at an earlier time, it is occurring at a time approach to 45 ns when the $n_i = 4 \times 10^{18} cm^{-3}$, while at $n_i = 3 \times 10^{18} cm^{-3}$, the steady state of losses occurs at 57 ns.

Figure 4**a, b** show the absorption activity for the ground state and excited state of SA, as well as the total absorption activity of the SA for wavelength $1.064 \mu m$ and 0.963 μm for $n_i = 3 \times 10^{18} cm^{-3}$ and $n_i = 4 \times 10^{18} cm^{-3}$. From the figure, can be seen that the absorption activity of the ground state decreases with time until it reaches a steady state, while the absorption activity of the excited state increases with time. The absorption activity of the excitation state and the ground state are equal at an earlier time when increase, can be observed at $n_i = 3 \times 10^{18} cm^{-3}$ the losses equal approximately at time 47 ns, while at $n_i = 4 \times 10^{18} cm^{-3}$ approximately at time 35 ns. Then the optical bleaching state occur at advance time when the SA ions density increases.

Figure 5**a, b** shows the absorption activity in the ground state and excitation level of SA, as well as the absorption activity of the SA for wavelength $0.946 \mu m$ for $n_i = 3 \times 10^{18} cm^{-3}$ and $n_i = 4 \times 10^{18} cm^{-3}$. From the figure, can be seen that the absorption activity of the ground level decreases with time until it reaches a steady state, while the absorption activity of the excited state increases with time. If the absorption activity of the excitation state and the ground state are equal, then the optical bleaching state occur at advance time when n_i increases.
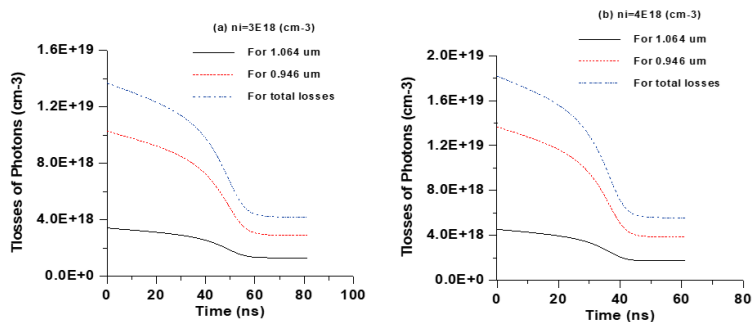
Fig 3. Profiles of photons losses as a function of time for two values of SA ions density
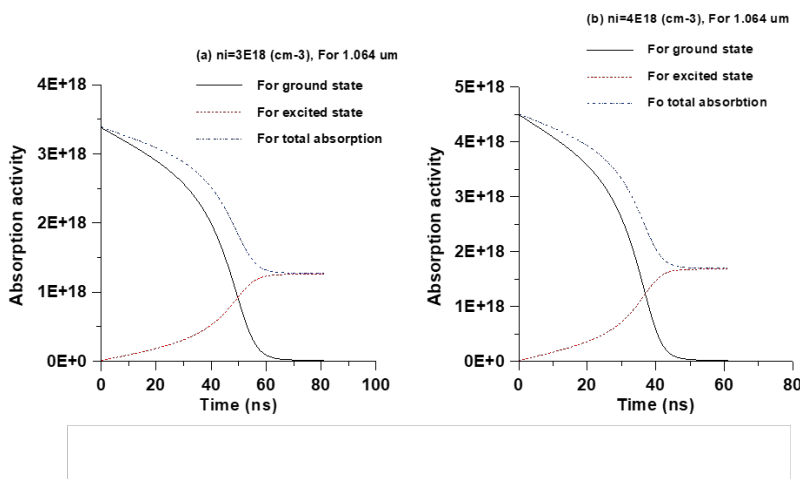
Fig 4. The behavior time of absorption activity of SA for ground, excited levels and total absorption, for $1.064\mu m$ for two values of SA ions density
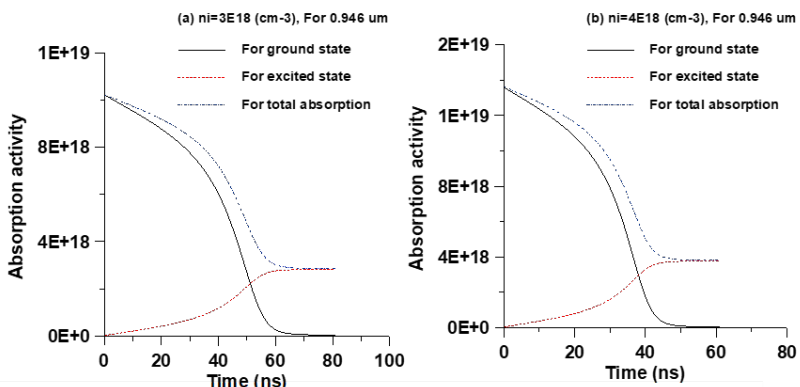
Fig 5. The behavior time of absorption activity of SA for ground, excited levels and total absorption, for $0.964\ \mu m$ for different SA ions density.

4 Conclusion

The study concludes the following: The temporal behavior of absorption activity of the SA towards each of the wavelength of dual wavelengths similar to the temporal behavior of a single wavelength which content of the studies [6,7], this supports the theoretical basis of this study. The steady state of losses occurs at an earlier time when SA ions density increases. The SA optical bleaching state for each wavelength occur at advance time when the n_i increases. The absorption activity of the ground state decreases with time until it reaches a steady state, while the absorption activity of the excited state increases with time. The absorption activity of the excitation state and the ground state are equal at an earlier time when n_i increase.

References

1) Zhang X, Zhong K, Qiao H, Zheng Y, Li F, Xu D, et al. A passively Q-switched dual-wavelength laser with pulsed LD coaxial end-pumped configuration. In: Advanced Lasers, High-Power Lasers, and Applications XIII;vol. 12310. SPIE. 2022;p. 24–30. Available from: https://doi.org/10.1117/12.2641747.

2) Wang J, Xie L, Wang Y, Lan Y, Wu P, Lv J, et al. High-damage vanadium pentoxide film saturable absorber for sub-nanosecond Nd:YAG lasers. *Infrared Physics & Technology*. 2023;129:104580. Available from: https://doi.org/10.1016/j.infrared.2023.104580.

3) Pérez-Alonso V, Weigand R, Sánchez-Balmaseda M, Pérez JMG. Powerful algebraic model to design Q-switched lasers using saturable absorbers. *Optics & Laser Technology*. 2023;164:1–13. Available from: https://doi.org/10.1016/j.optlastec.2023.109506.

4) Wang P, Zhu C. Passively Q-Switched and Mode-Locked Fiber Laser Based on a Zeolitic Imidazolate Framework-67 Saturable Absorber. *Frontiers in Physics*. 2022;10:1–8. Available from: https://doi.org/10.3389/fphy.2022.926344.

5) Li M, Qin Y, Wang C, Liu X, Long S, Tang X, et al. Nonuniform pumped passively Q-switched laser using Nd:YAG/Cr4+:YAG composite crystal with high-pulse energy. *Optical Engineering*. 2019;58(03). Available from: https://doi.org/10.1117/1.OE.58.3.036106.

6) Hussein TM, Salih AKM. Simulation of effective area ratio effect on saturable absorber absorption activity in passive Q-switching doped fiber laser system. *Advanced Engineering Science*. 2022;54(2):3041–3050. Available from: https://advancedengineeringscience.com/article/pdf/168.pdf.

7) Hussein ZA, Salih AK. Investigation of Initial Transmission Effect on Saturable Absorber Optical Performance of Passive Q-Switching Doped Fiber Laser. *NeuroQuantology*. 2021;19(7):103–109. Available from: https://www.neuroquantology.com/media/article_pdfs/103-109_NtQBwGQ.pdf.

8) Saad DH, Hussein H, Salih AM. Rate Equations Model to Simulate the Performance of Passive Q-Switched Laser with Raman Medium Optical System. *Indian Journal Of Science And Technology*. 2023;16(39):3353–3360. Available from: https://doi.org/10.17485/IJST/v16i39.1744.

9) Tang J, Bai Z, Zhang D, Qi Y, Ding J, Wang Y, et al. Advances in All-Solid-State Passively Q-Switched Lasers Based on Cr4+:YAG Saturable Absorber. *Photonics*. 2021;8(4):1–14. Available from: https://doi.org/10.3390/photonics8040093.

10) Tarkashvand M, Farahbod AH, Hashemizadeh SA. Study of the Spatiotemporal Behavior of LED-Pumped Ce:Nd:YAG Laser. *International Journal of Optics and Photonics*. 2020;14(1):75–84. Available from: https://ijop.ir/article-1-396-en.pdf.

11) Abdulhussain S, Salih AKM. Rate Equations Model to Simulate the Dual Generation of Nd+3: YAG Passive Q-swiched Laser Pulses. *Indian Journal of Science and Technology*. 2023;16(40):3462–3470. Available from: https://doi.org/10.17485/IJST/v16i40.1748.

12) Zhang B, Chen Y, Wang P, Wang Y, Liu J, Hu S, et al. Direct bleaching of a Cr4+:YAG saturable absorber in a passively Q-switched Nd:YAG laser. *Applied Optics*. 2018;57(16):4595–4600. Available from: https://doi.org/10.1364/AO.57.004595.

13) Giese A, Körber M, Kostourou K, Kopf D, Kottcke M, Lohbreier J, et al. Passively Q-switched sub-100 ps Yb3+:YAG/Cr4+:YAG microchip laser: experimental results and numerical analysis. In: Solid State Lasers XXXII: Technology and Devices;vol. 12399. SPIE. 2023;p. 187–197. Available from: https://doi.org/10.1117/12.2649057.

14) Gürel Ö. Development of a UV Source Based on Frequency Quadrupling of a Q-switched Nd:YAG laser. Stockholm, Sweden. 2009. Available from: https://www.aphys.kth.se/polopoly_fs/1.422571.1600689849!/Menu/general/column-content/attachment/G%C3%BCrel_msc_thesis_2009.pdf.

15) Li M, Qin Y, Wang C, Liu X, Long S, Tang X, et al. Nonuniform pumped passively Q-switched laser using Nd:YAG/Cr4+:YAG composite crystal with high-pulse energy. *Optical Engineering*. 2019;58(03). Available from: https://doi.org/10.1117/1.OE.58.3.036106.

16) Koechner W. Solid-State Laser Engineering;vol. 1 of Springer Series in Optical Sciences. Heidelberg, Germany. Springer Berlin. 1988. Available from: https://doi.org/10.1007/978-3-662-15143-3.

17) Tang J, Bai Z, Zhang D, Qi Y, Ding J, Wang Y, et al. Advances in All-Solid-State Passively Q-Switched Lasers Based on Cr4+:YAG Saturable Absorber. *Photonics*. 2021;8(4):1–14. Available from: https://doi.org/10.3390/photonics8040093.